



HAL
open science

Comparative study of thermal radiation properties models in turbulent non-premixed sooting combustion

E. Orbegoso, L. Figueira da Silva, R. Serfaty

► **To cite this version:**

E. Orbegoso, L. Figueira da Silva, R. Serfaty. Comparative study of thermal radiation properties models in turbulent non-premixed sooting combustion. Numerical Heat Transfer, Part A Applications, 2015, 69 (2), pp.166-179. 10.1080/10407782.2015.1052318 . hal-03313652

HAL Id: hal-03313652

<https://hal.science/hal-03313652>

Submitted on 26 Jul 2022

HAL is a multi-disciplinary open access archive for the deposit and dissemination of scientific research documents, whether they are published or not. The documents may come from teaching and research institutions in France or abroad, or from public or private research centers.

L'archive ouverte pluridisciplinaire **HAL**, est destinée au dépôt et à la diffusion de documents scientifiques de niveau recherche, publiés ou non, émanant des établissements d'enseignement et de recherche français ou étrangers, des laboratoires publics ou privés.

**COMPARATIVE STUDY OF THERMAL RADIATION
PROPERTIES MODELS IN TURBULENT NON PREMIXED
SOOTING COMBUSTION**

E. M. Orbegoso*, L. F. Figueira da Silva* and R. Serfaty**

**Departamento de Engenharia Mecânica, Pontifícia Universidade Católica do Rio de Janeiro, Rua Marquês de São Vicente 225, Gávea, CEP 22451-000, Rio de Janeiro, Brasil.*

***Centro de Pesquisa, Petróleo Brasileiro S.A., Avenida Horácio Macedo, 950, Cidade Universitária, Ilha do Fundão, Gávea, CEP 21941-915, Rio de Janeiro, Brasil.*

eldermendoza_24@hotmail.com, luisfer@esp.puc-rio.br, rserfaty@petrobras.com.br

COMPARATIVE STUDY OF THERMAL RADIATION MODELS IN TURBULENT NON PREMIXED SOOTING COMBUSTION

This work presents a numerical study of radiation heat transfer and its interaction with gray and spectral radiation of combustion products and soot that are formed in a turbulent non-premixed combustion process. To this purpose, WSGGM, Rayleigh, Narrow-Band Model and semi-empirical radiation properties models are considered. Two situations are studied, 1-D radiation problem and non-premixed gaseous combustion process. The results demonstrate that models exhibit discrepancies that are smaller than available line-by-line or experimental data. A study of the factors which influences such a disagreement is presented, underscoring the role of chemical kinetics of hydrocarbon species and of soot oxidation.

Keywords: Computational fluid dynamics, Non-premixed turbulent combustion, Radiative transfer equation, Soot radiation properties.

I. Introduction

Industry activities require huge amount of heat in their processes. Typically, fired heaters, boilers, furnaces, dryers and other equipment use combustion as major source of energy. In these equipments, a significant amount of heat released is transferred to the feed by radiation. The accurate prediction of such a heat transfer rate profile is of paramount importance, for instance, to increase the run length time for process units as for refining and reheating furnaces [1]. In these equipments radiative heat transfer is ensured both by gaseous combustion products, such as carbon monoxide, carbon dioxide, water vapor, and by soot [2]. Since combustion temperatures are extremely high, thermal radiation often plays a crucial role when compared to other energy transfer mechanisms as conduction and advection.

Therefore, the accurate prediction of these combustion products, as well as their radiative properties, should lead to a good characterization of flames, and the associated transfer mechanism, and also the accurate prediction of pollutants formation within such systems. It is important to highlight that pollutant emission are also a crucial point for industrial application, due to increasingly restrictive environment laws for this kind of service. In order to improve accuracy on local heat transfer and pollutant formation predictions, more complex models must be used.

Furthermore, another severe restriction on this scenario is related to the difficulty of obtaining good experimental results in order to validate numerical and mathematical models of such industrial equipments. Even for pilot plants it is really difficult to get all experimental results required for a serious validation process of these models, including radiation on participating media with soot formation for the combustion of industrial fuels.

The development of computationally tractable models of such transfer processes, which could be used as analysis and optimization tools for industrial purposes [1], require the understanding of the predictive capability of each sub model used.

The present study is part of an endeavor which aims to develop such a tool. The main objective of this study is to assess the predictive capability of existing and implemented models over physical situations in which parametrical analysis is performed. This analysis investigates the influence of the choice of radiation model for gaseous species and soot on the results obtained for: (i) a canonical configuration for which exact results are available and (ii) a turbulent enclosed flame jet, where soot and radiation measurements exist.

The computational fluids dynamics (CFD) simulation for these studies uses the Reynolds Averaging Navier-Stokes (RANS) approach together with flamelet model and radiation property models and soot formation, in order to numerically describe the complex aero-thermochemical process that comes about in the operation of such industrial combustion equipment's. The radiation property models used in this work are

both weighted sum of grey gases and narrow band models. To the best of the authors' knowledge, such detailed comparisons are absent from the literature.

II. Numerical Methodology

2.1 Thermal radiation modeling

Classically, thermal radiation is transferred via discrete packets of energy, i.e., photons, mostly on the infrared spectrum wavelength (0.1 - 100 μm). The variation of thermal radiation intensity in quasi-steady state that crosses a participant medium which absorbs, scatters and emits radiant energy is described by radiative transfer equations (RTE) that, under the spectral and gray assumption, are given by [3],

$$\frac{dI_\lambda(\vec{r}, \vec{s})}{ds} = -(a_\lambda + \sigma_{s,\lambda})I_\lambda(\vec{r}, \vec{s}) + a_\lambda n^2 I_{\lambda,b}(\vec{r}) + \frac{\sigma_{s,\lambda}}{4\pi} \int_0^{4\pi} I_\lambda(\vec{r}, \vec{s}') \Phi(\vec{s}, \vec{s}') d\Omega', \quad (1)$$

$$\frac{dI(\vec{r}, \vec{s})}{ds} = -(a + \sigma_s)I(\vec{r}, \vec{s}) + an^2 \sigma \frac{T^4}{\pi} + \frac{\sigma_s}{4\pi} \int_0^{4\pi} I(\vec{r}, \vec{s}') \Phi(\vec{s}, \vec{s}') d\Omega', \quad (2)$$

where $dI_\lambda(\vec{r}, \vec{s})$ and $dI(\vec{r}, \vec{s})$ are the spectral and gray intensities of radiant energy at a given location \vec{r} , in a beam traveling in direction \vec{s} . $I_{\lambda,b}(\vec{r})$ is the spectral intensity of radiation emitted by a blackbody which expression is given by the Planck function, $a_\lambda = a_{\lambda,g} + a_{\lambda,soot}$ and $a = a_g + a_{soot}$ are the spectral and gray absorption coefficients of the gas ($a_{\lambda,g}, a_g$) and soot ($a_{\lambda,soot}, a_{soot}$), $\sigma_{s,\lambda}$ and σ_s are the spectral and gray scattering coefficients of the medium, n is the complex refractive index, σ is the Stefan-Boltzman constant, $5.67 \times 10^{-8} \text{ W/m}^2\text{K}^4$, T is the medium temperature, $\Phi(\vec{s}, \vec{s}')$ is the scattering phase function and Ω' is the solid angle.

In Eqs. (1)-(2), the first term on the right hand side describes the reduction of the intensity along a prescribed direction due to absorption by the participant medium or due to scattering in other directions. The second term corresponds to the increase in the intensity due to thermal emission by the medium, and the last term is relevant only if the medium scatters radiation. The phase function, $\Phi(\vec{s}, \vec{s}')$, describes the probability of a ray

which comes from a direction \vec{s}' to scatter on a direction \vec{s} . For the case when a participant medium comprises gas of combustion products and low concentrations of soot, the effect of scattering can be neglected without incurring a loss of accuracy in the calculation of thermal radiation [4].

Several methods have been developed in order to solve the RTE [Eqs. (1)-(2)]. These methods include various analytical approaches, such the P1 model [5], as well as numerical methods, like the Discrete Ordinates Model, (DOM) [6]. The numerical calculation of thermal radiation transferred in non-homogenous and non-isothermal medium, as is the case of combustion processes, requires the solution of thousands of discretized spectral radiative transfer equations [Eq. (1)]. This process demands a computational burden that is impossible to reach in the context of CFD simulation of practical engineering systems. Even for homogenous and isothermal medium, the numerical solution of the spectral RTE demands a significant computational effort [7].

Even with the gray medium assumption [Eq. (2)], the solution of the RTE is a challenge from the computational point of view. Indeed, it is necessary not only to solve the radiative transfer equation as a function of Cartesian and angular coordinates, but to account for the complex wavelength dependence of the participant medium radiant properties [4]. Thus, the radiation modeling involves (i) the solution of the radiative transfer equation and, (ii) determining the participating medium radiant properties.

Several approaches have been developed in order to account for the variation of spectral radiant properties of combustion products gases. The choice of the model to be used depends on the application and the required degree of accuracy. In many situations, the appropriate choice is the result of the competition between accuracy and computational cost. These approaches may be grouped in three categories, (i) line-by-line (LBL), (ii) Narrow Band Models (NBM) and, (iii) global models that are based primarily on the concept of Weighted Sum of Gray Gases (WSGGM).

The LBL approach is the most accurate one for the calculation of gaseous participating medium thermal radiation. In this model, the spectral radiative transport equation [Equation (1)] is integrated over the molecular spectra [8]. Since the radiant

properties of the combustion products gases vary strongly through the wavelength spectrum, its accurate solution needs to consider thousands of spectral lines and bands. Their discretization and numerical solution takes into account thousands of spectral radiative transport equations that involves difficulties related to their implementation and computational burden.

The NBM approach approximates the average behavior of the spectral absorption coefficient over a small range of wavelengths. Analytical expressions arise for the spectral transmissivity, τ_λ , which is weighted over a small enough wavelength band, $\Delta\lambda$, where the spectral intensity of the black body, $I_{b,\lambda}$, is assumed to be constant. Since hundreds of absorption lines can be contained within a wavelength band, various statistical and analytical assumptions are made in order to determine the equivalent transmissivity in each spectral interval. The typical spectral domain of NBM approach for determining the spectral radiant properties of CO₂-H₂O mixture lies between 1.43 and 67 μm . This requires the distribution of at least 300 narrow bands regions. Therefore, the complexity and computational effort of NBM approach still does not render it sufficiently attractive for engineering application purposes. Nevertheless, this approach is commonly used for validation purposes [4]. Several computer codes, such as Radcal [9] and MS2C [10], determine the radiant properties of gaseous combustion products using the NBM approach.

On the other hand, there are several soot radiation properties models with various accuracy and sophistication levels, ranging from spectral models, such as the Dobbins et al [11] model and the Rayleigh theory [3] to global [12] or empirical [13] ones.

The determination of the spectral soot radiant properties requires the knowledge of thermochemical (temperature and concentration) and optical (particle shape and size distribution, complex refraction index, wavelength, etc.) soot properties. This is a complicated task due to the complexity the soot structure. The Rayleigh absorption/scattering theory describes the attenuation of a light beam passing through a cloud of monodispersed or polydispersed spherical particles. In this theory, the soot volume fraction, f_V , the soot diameter, d_p , and soot complex refractive index, m , allow to obtain the spectral absorption, $a_{\lambda,soot}$ and scattering, $\sigma_{\lambda,soot}$ coefficients [3] and may

be used to determine soot radiative properties. The Radcal code [9] simplifies the Rayleigh theory in order to determine the soot spectral absorption coefficient, $a_{\lambda,soot}$, as a function of soot volume fraction. Soot scattering is not accounted for. The Planck and Rosseland integrations of the spectral absorption coefficient over the wavelength spectra lead to global mean absorption that depend on soot volume and temperature only. These global coefficients are commonly used for engineering purposes to determine the soot radiant transport.

Empirical radiant properties models based on experimental results couple the soot production with the radiant transport in a simple manner, thus requiring little processing time and being amenable for engineering applications. The Sazhin [13] model relates the soot global absorption coefficient, a_{soot} , to the soot volume fraction and temperature.

On the following, the WSGGM(Smith) [14], WSGGM(Mossi) [7], Sazhin [13], Rayleigh theory [3] and NBM(Radcal) [9] radiation properties models and their coupling with Moss Brookes [15] soot production model are used in two scenes in order to assess those that better predicts the combustion products and soot radiative transport from a CFD perspective.

The two configurations studied in this work have been chosen since they allow for parametrical analysis which would otherwise be impossible in actual furnaces. These configurations exhibit the essential features of the radiation heat transfer occurring in practical devices. The canonical configuration of the hot combustion products between planes has been solved by a line-by-line method [7], which provides essentially an exact solution for comparison purposes. The second configuration studied is an enclosed flame jet that contains the basic ingredients of mass, momentum and heat transfer, as well as soot formation and oxidation.

2.2 The non-isothermal homogeneous flat plates

Several CO₂-H₂O and soot radiant properties models are considered in order to determine the one that yields the best agreement with the divergent of the radiant heat flux, $-\nabla \cdot \vec{q}_r$. Therefore, are used, (i) the WSGGM approach [16], with temperature

dependent coefficients obtained from the works of Smith *et al.* [14] [WSGGM(Smith) model] and Mossi [7] [WSGGM(Mossi) model] and, (ii) the NBM approach, through the Radcal code [9] [NBM(Radcal) model]. The radiant properties of soot are calculated by (i) the Sazhin [13] semi-empirical formula [Sazhin model], (ii) the absorption/scattering Rayleigh theory [3] [Rayleigh model] and, (iii) the NBM(Radcal) model [9].

The configuration on which such models are compared is the homogeneous and non-isothermal gas mixture composed of 10% (by mass) of CO₂, 10% of H₂ and 80% of N₂, confined between two parallel flat plates separated by $L = 1$ m and which temperature is maintained at $T_P=500$ K. The temperature of the mixture is prescribed as $T(y) = 2000 - 1500(2y/L-1)^2$.

Concerning the study of the influence of soot radiant properties models, 1% of uniformly distributed monodispersed spherical 18 nm diameter soot particles replaces 1% of N₂. The complex index of refraction is assumed in accordance to the Chang and Charampopoulos [17] formulae.

2.3 The Endrud Non-Premixed Burner

The Endrud [18] burner is composed of a vertically mounted circular duct of 200 mm diameter and 1150 mm length. Propane, C₃H₈, is injected through a 3 mm diameter duct at 300 K and 21.8 m/s ($Re = 15\ 000$). The oxidizer, i.e., oxygen enriched air (40% O₂ and 60% N₂) at 300K and 0.6 m/s, is concentrically fed to the burner (coflow). Note that the inner burner wall has an internal emissivity that is considered equal to that of a black-body.

Fig. 1 shows the discretized computational domain used for the Endrud [18] burner combustion process simulation. In this figure it may also be observed that the computational domain corresponds to a circular region of 6° . This aims to reduce, under revolution symmetry assumption, the computational burden associated to the simulation of the complete configuration.

In the turbulent combustion modeling, the transport equations for mass, momentum and energy are used in the context of classical Reynolds Averaged Navier

Stokes (RANS). The realizable k- ϵ model [19] is considered to describe the turbulent transport. In addition, the non-adiabatic flamelet model [20] is used to represent the non-premixed turbulent combustion together with the GRI-Mech 3.0 [21] to describe propane/air combustion kinetics. A recent assessment of the predictive capability of several chemistry mechanisms may be found elsewhere [22]. The Discrete Ordinates Model (DOM) allows the discretization of the radiative transfer equation (RTE) into finite solid angles [6]. The radiant properties of CO₂-H₂O gases are obtained by applying the WSGGM(Smith) [14], WSGGM(Mossi) [7] and NBM(Radcal) [9] models. Note that the use of this NBM requires the coupling between Radcal and FluentTM, which is the computational fluid dynamic code used.

The Moss-Brookes soot model [15] is used to describe the soot production. This model accounts for the competition between the process of nucleation, surface growth, agglomeration and oxidation. Such a model relies on the chemical kinetic mechanism to predict the acetylene concentration, C₂H₂, which in turn leads to the formation of soot. The hydroxyl radical, OH, is the responsible for soot oxidation. Finally, Sazhin [13], Rayleigh [3] and NBM(Radcal) [9] models allow for the coupling between radiation and soot. These models determine the radiant properties of soot as a function, among other parameters, of the soot volume fraction.

The specific boundary conditions used are presented in Table 1. In this table, $U_{z,0}$ is the longitudinal velocity at the entrance of the reactants, $X_{C_3H_8}$, X_{O_2} and X_{N_2} , are the propane, oxygen and nitrogen mole fractions, \bar{Z} and $\widetilde{Z''^2}$ are the mean and the variance of the mixture fraction, I_t is the turbulent intensity, defined as the ratio between the absolute value of the turbulent fluctuations of the velocity field and the mean velocity, l_t is the integral length scale characteristic of turbulence.

III. Results and Discussion

3.1 The non-isothermal homogeneous flat plates

Fig. 2a shows the divergent of radiant heat flux, $-dq_r/dy$, between the two flat

plates when WSGGM(Smith), WSGGM(Mossi) and NBM(Radcal) models are used for the description of CO₂-H₂O radiant properties. The computed results are compared with those obtained by Mossi [10] using the baseline LBL-HITEMP approach. The overall tendencies are similar, i.e., all results exhibit minimum values at the center ($y = 0.5$ m) and maximum near the planes. In particular, at the symmetry plane ($y=0.5$ m), WSGGM and NBM models show similar results where, the largest discrepancy observed is 38 kW/m³, i.e., 9%. Nevertheless, none of the three models correctly reproduces the LBL-HITEMP results.

An analysis of the central region ($0.25 < y < 0.75$ m), Fig. 2a also shows that WSGGM models are those that better represent the LBL-HITEMP results, when compared to NBM(Radcal) model. The discrepancies with respect to the LBL-HITEMP results associated to WSGGM(Smith) and WSGGM(Mossi) models do not overcome 13 and 16%, respectively. Near the plate ($y < 0.25$ and $y > 0.75$ m), none of the three models is able to reproduce with good accuracy the divergent of radiant heat flux. It is important to emphasize that similar discrepancies were also reported by Mossi [10], when WSGGM models were used. It should be emphasized that the computational cost of the NBM(Radcal) model is about 30 times larger than that of the WSGGM models.

The results of the divergent of the radiant heat flux profile, $-dq_r/dy$, given in the Fig. 2b for the three models considered allow to compare the different CO₂-H₂O and soot radiant properties. Indeed, a good agreement of $-dq_r/dy$, between NBM(Radcal) and WSGGM(Smith)&Sazhin models is verified throughout the domain. Small discrepancies, that do not exceed 6%, are observed in the entire domain. On the other hand, near wall the WSGGM(Smith)&Rayleigh model leads to $-dq_r/dy$ values that underestimate, up to 30%, the results obtained by WSGGM(Smith)&Sazhin and NBM(Radcal) models. In the central region, the values obtained by the WSGGM(Smith)&Rayleigh and WSGGM(Smith)&Sazhin models differ by 9%. These results indicate the successful implementation of the Rayleigh model and the coupling Radcal/Fluent routines on the implementation of the NBM(Radcal) model.

Figures 3, 4 and 5 depict, for the different radiation models, the influence of the choice of the mean pathlength, L_m , over the divergent of the radiant heat flux, $-dq_r/dy$,

the incident radiation, G , and the global absorption coefficient, a . The homogeneous and non-isothermal gas mixture composed of 10% (by mass) of CO_2 , 10% of H_2 and 80% of N_2 is considered, i.e., without the inclusion of soot. At the computed results exhibit similar trends, with maximum values of incident radiation and minimum absorption coefficient at the center ($y=0.5\text{m}$).

Fig. 3 shows a good agreement between NBM(Radcal) and LBL-HITEMP results, when the mean pathlength, L_m , is equal to $1.5L$. Also, the WSGGM(Mossi) model reproduces the LBL-HITEMP results, when $L_m = 1.8L$. It is noticed that, for the same L_m , the WSGGM(Smith) overpredicts a maximum of 10% the NBM(Radcal) results. For any specific model, the increase of L_m from $1.5L$ to $1.8L$, leads to the increase of $|\frac{dq_r}{dy}|$ profile at a maximum of 8%. None of the models exactly represent the LBL-HITEMP results.

A similar behavior is observed in Fig. 4, where the incident radiation profile is observed to increase with L_m . Also, is verified that, for the same mean pathlength, the incident radiation obtained by the WSGGM(Smith) always overestimates that of the NBM(Radcal) model. The NBM(Radcal) model with $L_m = 1.5L$ gives values of G that are similar to those obtained by the WSGGM(Smith) model at $L_m = 1.8L$.

The gas global absorption coefficient, $a = a_g$, obtained by the WSGGM(Smith) and NBM(Radcal) models are shown in Fig. 5. For the NBM(Radcal) model the decrease of L_m from $1.8L$ to $1.0L$ yields to an increase of the gas global absorption coefficient up to 34%. A similar behavior is observed for the WSGGM(Smith) model where, i.e., an increase up to 38% is found when L_m is reduced from $1.8L$ to $1.0L$.

It may be observed in Fig. 5 that the NBM(Radcal) model exhibits a non-monotonic behavior, i.e. a maximum of a gas mean absorption coefficient is located at 0.05 m from the flat plates. This behavior seems to be intrinsic to the NBM(Radcal) model, where the gas radiant properties are related to the competition between global radiation intensity and the mean effective absorption-emission coefficient given by $I =$

$$\frac{\sigma}{\pi} [(1 - \exp(-a_E L_m))T^4 + \exp(-a_E L_m)T_P^4].$$

The results discussed at this section clearly show that none of gray models accurately reproduce the LBL results, which effectively limits what could be expected when comparisons with experimental data are of interest.

3.2 The Endrud Non-Premixed Turbulent Burner

In this section the Endrud [18] non-premixed turbulent burner is considered in order to investigate the predictive capacity of CO₂-H₂O and soot radiant property models that were accounted for this work. To this end, a comparison is developed between Wang *et al.* [23, 24, 25] experimental data of radiant heat flux, q_r , and equivalent soot volume fraction F_V^* , and the corresponding numerical results obtained with the WSGGM(Smith) and WSGGM(Smith)&Sazhin models. These results are also compared against numerical results of Wang *et al.* [25]. This comparison is then extended to WSGGM(Smith)&Sazhin, WSGGM(Smith)&Rayleigh and NBM(Radcal) models. The experimental results exhibit coincident maximum values of radiant heat flux and soot volume fraction at $z = 0.5\text{m}$. This non-monotonic behavior is also found at the computations, albeit with different values and locations.

Fig. 6 shows the results obtained using the WSGGM(Smith) model, for the calculation of radiant properties of gaseous products and the WSGGM(Smith)&Sazhin, which determines the radiant properties of gaseous products and soot. These results are compared with the P1-Full Spectrum κ -model (P1-FSK) and P1-Full Spectrum κ -model with Moment Method (P1-FSK&MM) obtained by Wang *et al.* [25] and, also, to the measurements of Wang *et al.* [24, 25].

In cases where soot formation is not accounted for, Fig. 6a shows that the radiant heat flux obtained with the WSGGM(Smith) model leads to a better agreement with measurements than those of Wang *et al.* [24, 25] which used the P1-FSK model. Moreover, the WSGGM(Smith) model slightly underestimates the experiments near $z = 0$, whereas the P1-FSK model overestimates, up to six times, the values of radiant heat flux, q_r . According to Wang [24], the main reason for the discrepancy is the overestimation of the temperature field with the Eddy Break-Up combustion model used. Indeed, this model

provides high reaction rates, and hence, temperatures that are close to equilibrium. Another possible explanation for this discrepancy could be the intrinsic limitation of the P1 radiation model to predict the radiant transport on participating medium with small optical thickness. Note that the optical thickness near the entrance does not exceed 0.1. The overestimation of radiant heat flux in regions that are close to the exit is addressed below. In cases where the radiant soot properties are accounted for, the results obtained with the WSGGM(Smith)&Sazhin model lead, when compared with experimental data, to a better representation of the peak value of the radiant heat flux q_r than the P1-FSK&MM. However, the WSGGM(Smith)&Sazhin model exhibits an upstream displacement of this peak value, when compared to the experimental data. This discrepancy seems to be directly related to the location of the maximum soot concentration, which is dependent on the interaction between the turbulence, combustion, radiation and soot production models. Indeed, Fig. 6b shows the results of the equivalent soot volume fraction computed, F_V^* , obtained with the WSGGM(Smith)&Sazhin model, those computed by Wang *et al.* [25] using the P1-FSK&MM model and the experiments. Note that, for $z < 330$ mm, the WSGGM(Smith)&Sazhin model leads to a better prediction of F_V^* than the P1-FSK&MM model. Both models exhibit a maximum of F_V^* that reaches 8.5 ppm (at $z = 330$ mm) and the same downstream decay rate, as a consequence of the soot oxidation. It is noteworthy that, for $z < 330$ mm, both WSGGM(Smith)&Sazhin and P1-FSK&MM models correctly reproduce the experimental data of Wang *et al.* [24, 25].

The comparison of the WSGGM(Smith)&Sazhin, WSGGM(Smith)&Rayleigh and NBM(Radcal) with the measurements of Wang *et al.* [24, 25] of radiant heat flux, q_r , and equivalent soot volume fraction F_V^* , is shown in Fig. 7. Concerning to q_r , these three models yield a similar profile, with differences on the maximum values, and similar upstream displacement of these extreme. The WSGGM(Smith)&Rayleigh model overestimates the experiments in 20%. The NBM(Radcal) model provides a q_r distribution which maximum does not overcome 9% the experimental data.

Regarding the evolution of the equivalent soot volume fraction, F_V^* , the comparison of computed and experimental results shows that all models considered in here lead to better estimates of F_V^* than the P1-FSK&MM model. Furthermore, the

studied models reproduce the gradients of soot formation and oxidation. The NBM(Radcal) is the model that best represents the soot production, in particular, the maximum value of F_V^* , is only 25% lower than that obtained in Wang *et al.* [24, 25] experiments. On the other hand, the maximum of F_V^* predicted by WSGGM(Smith)&Sazhin and WSGGM(Smith)&Rayleigh models are, respectively, 50 and 67% of that measured.

In order to analyze soot production and oxidation, Fig. 8 shows the contours of (i) soot volume fraction, (ii) its precursors in the formation (C_2H_2) and oxidation (OH), and (iii) the surface , growth, oxidation and overall soot rate. In this case, the WSGGM(Smith)&Sazhin model has been considered for the global radiant properties determination of combustion products and soot, and where the Moss-Brookes [15] model is used for the soot production. As may be verified in Fig. 8a, the soot production begins near $z = 230$ mm, which is the location where maximum concentrations of acetylene (C_2H_2) are also evidenced. This reflects the fact that in the soot model used [15] is governed by the competition between the soot formation (inception, and grow surface) and oxidation rates, where the acetylene and the hydroxyl are the precursor and oxidant species, respectively. The maximum soot concentration is located near $z = 350$ mm, downstream to which the acetylene concentration decreases. At the end region, soot is consumed due to the hydroxyl predominance over acetylene. This discussion may be extended examining the evolution of acetylene and hydroxyl in Fig. 8c-e, where are shown: (i) mass rate soot formation by surface growth, (ii) mass rate of soot oxidation and, (iii) overall soot production rate. The comparison between Fig 8c and Fig 8d shows that, in the region bounded by $250 < z < 400$ mm and near to symmetry axis, the soot production process is mainly governed by surface growth. A balance of all the contributions to the soot surface growth and oxidation processes is depicted in Fig. 8e, where two different regions may be observed:

- A region of positive values of overall soot rate (soot production) between $250 < z < 400$ mm and $-16 < y < 0$ mm.
- Soot consumption and oxidation region in which, negative values of overall soot rate are observed between $100 < z < 1063$ mm and $-100 < y < -20$ mm.

The influence of the oxidation scaling parameter, C_{oxid} of Moss-Brookes [15] model, on the radiant heat flux and the equivalent soot volume fraction may be examined in Fig. 9. In this case, the WSGGM(Smith)&Sazhin and NBM(Radcal) have been considered, and values of C_{oxid} equal to 0.8 (original) and 0.4 (modified) have been used. Note that the latter has been adopted with the purpose of delaying oxidation.

The reduction of C_{oxid} to 0.4 leads to an overall increase of the radiant heat flux, q_R , by approximately 60% for both radiation models. Note that C_{oxid} reduction yields an overprediction of Wang [25] experimental results.

Concerning the equivalent soot volume fraction, F_V^* , for the WSGGM(Smith)&Sazhin model, the use of C_{oxid} equal to 0.4 leads to an increase of 70% of this property. Moreover, may be observed that the coupling of Moss-Brookes model with the WSGGM(Smith)&Sazhin model leads to values of, F_V^* , that are comparable to those measured by Wang [25], however, the reduction of C_{oxid} does not allow to reproduce the soot formation and consumption rates. A similar behavior is evidenced for the NBM(Radcal), where this reduction of C_{oxid} yields to a reduction of 25% for the maximum F_V^* value, when compared with the Wang [25] experimental results.

It could be suggested that a combined parametrical study of all Moss-Brookes constants [15], such as the scaling parameter of oxidation, C_{oxid} , and the surface growth rate scaling factor, C_γ , would lead a better agreement with the experimental measures of q_R and F_V^* . However, this has not been attempted here.

The influence of the CO₂-H₂O and soot radiation models on the global thermochemical properties is given in Table 2, which shows the comparison of the total, $\dot{Q}_{T,P}$, and radiation, $\dot{Q}_{r,P}$, heat transfer rates, that are transferred from the flow to the burner wall. In this table, one can observe that the WSGGM(Smith)&Rayleigh model leads to a radiation heat transfer rate, $\dot{Q}_{r,P}$, that is 30% higher than measured by Wang *et al.* [23]. The WSGGM(Smith)&Sazhin and NBM(Radcal) models yield values of radiation heat transfer rate that are similar and smaller than that obtained with the

WSGGM(Smith)&Rayleigh model. Nonetheless, both models exhibit values of $\dot{Q}_{r,P}$, that are 22% higher than those measured. It is believed that choosing the values of wall temperature and emissivity to $T_P = 400$ K and $\varepsilon_P \approx 0.9$ could lead to computed results of, $\dot{Q}_{r,P}$, closer to those found in the experiments. Since the radiative heat transfer rate, $\dot{Q}_{r,P}$, comprises 90% the total heat transfer rate, $\dot{Q}_{T,P}$, the variation of the former strongly influences on the latter. Table 2 shows that the total heat transfer rate obtained with the WSGGM(Smith)&Rayleigh model is about 6% higher than those computed with the other models. This implies, only, an average temperature variation of 10 K at the exit of the computational domain.

IV. Conclusions

In this work was studied the influence that exert several CO₂-H₂O and soot radiant properties models on radiant energy transport and thermochemical properties of the participating medium. Two situations were analyzed, i.e., a homogeneous and a non-homogeneous system.

The first one, the heat transfer in homogeneous mixture between flat planes, show that none of different radiation models studied exactly reproduce the LBL results of heat flux divergent. Indeed, the discrepancy between models is smaller than that corresponding to the exact (LBL) results. Such a discrepancy could not be attributed to the choice of mean path length, even if its value was show to influence both the incident radiation and the absorption coefficient.

The second situation studied was a non-premixed turbulent burner. The WSGGM(Smith)&Sazhin, WSGGM(Smith)&Rayleigh and NBM(Radcal) models were compared with experimental data. These models were shown to represent the initial phase of soot formation and the corresponding heat flux width similar accuracy. However, the computed values of sot volume fraction is smaller than the measured none, which results in a premature soot disappearance in the computations. Furthermore, the predicted heat flux decrease is slower than the measurement. The first of these discrepancies could be

attributed to the soot formation model used, whereas the second did not seem to be connected to the soot oxidation rate.

As a final remark it should be noted that the obtained results strongly depend on combustion chemistry and soot production models. The results also suggest that the combined use of more sophisticated combustion chemistry and soot models, which involve other soot precursors, such as benzene, and oxidizers, such as atomic oxygen, could improve the quality of predictions.

V. Acknowledgement's

This research has been supported by Petrobras while Luís Fernando Figueira da Silva was on leave from the Institut Pprime (Centre National de la Recherche Scientifique, France).

VI. References

1. C. T. Hsieh, M. J. Huang, S. T. Lee, and C. H. Wang, A Numerical Study of Skid Marks on the Slabs in a Walking-beam Type Slab Reheating Furnace, *Numerical Heat Transfer, Part A: Applications*, vol. 57(1), pp. 1-14, 2010.
2. D. Poitou, J. Amaya, and F. Duchaine, Parallel Computation for Radiative Heat Transfer using the DOM in Combustion Applications: Direction, Frequency, Subdomain Decomposition and Hybrid Methods, *Numerical Heat Transfer, Part B: Fundamentals*, vol. 62(1), pp. 28-49, 2012.
3. M. Modest, *Radiative Heat Transfer*, 3rd ed., Academic Press, Oxford, 2013.
4. G. H. Yeoh, and K. K. Yuen, *Computational Fluid Dynamics in Fire Engineering - Theory, Modeling and Practice*, 1st ed., Academic Press, Oxford, 2009.
5. J. H. Jeans, The Equations of Radiative Transfer of Energy, *Monthly Notices Royal Astronomical Society*, vol. 78, pp. 28–36, 1917.

6. S. Chandrasekhar, *Radiative Transfer*, 1st ed., Dover Publications, New York, 1960.
7. A. Mossi, M. M. Galarça, R. Brittes, H. A. Vielmo, and F. H. R. França, Comparison of Spectral Models in the Computation of Radiative Heat Transfer in Participating Media composed of Gases and Soot, *Journal of the Brazilian Society of Mechanical Sciences & Engineering*, vol. 34(2), pp.112-119, 2012.
8. M. N. Ozisik, *Radiative Transfer and Interactions with Conduction and Convection*, 1st ed., Wiley, New York, 1974.
9. W. L. Grosshandler, Radcal: A Narrow-Band Model for Radiation Calculations in a Combustion Environment, National Institute of Standards and Technology, NIST Technical Report 1402, Washington, 1993.
10. A. Soufiani, and J. Taine, High Temperature Gas Radiative Property Parameters of Statistical Narrow-Band Model for H₂O, CO₂ and CO, and k-Correlated Model for H₂O and CO₂, *International Journal of Heat and Mass Transfer*, vol. 40(4), pp. 987–991, 1997.
11. R. Dobbins, G. Mulholland, and N. Bryner, Comparison of a Fractal Smoke Optics Model with Light Extinction Measurements, *Atmospheric Environment*, vol. 28(5), pp. 889–897, 1994.
12. A. Przybylski, On the Mean Absorption Coefficient in the Computation of Model Stellar Atmospheres of Solar Type Stars, *Royal Astronomical Society*, vol. 120(1), pp. 1-21, 1960.
13. S. S. Sazhin, An Approximation for the Absorption Coefficient of Soot in a Radiating Gas, Manuscript- Fluent Europe Ltd., 1994.
14. T. F. Smith, Z. F. Shen, and J. N. Friedman, Evaluation of Coefficients for the Weighted Sum of Gray Gases Model, *Journal of Heat Transfer*, vol. 104(4), pp. 602–608, 1982.
15. S. J. Brookes, and J. B., Moss, Predictions of Soot and Thermal Radiation Properties in Confined Jet Diffusion Flames, *Combustion and Flame*, vol. 116, pp. 486–503, 1999.

16. H. C. Hottel, and A. F. Sarofim, *Radiative Transfer*, 1st ed., Mc Graw Hill, New York, 1967.
17. H. Chang, and T. Charalampopoulos, Determination of the Wavelength Dependence of Refractive Indices of Flame Soot, *Proceedings of the Royal Society London*, vol. 430, pp. 577–591, 1990.
18. N. E. Endrud, Soot, Radiation, and Pollutant Emissions in Oxygen-Enriched Turbulent Jet Flames, Msc. Thesis, The Pennsylvania State University, Pennsylvania, Pennsylvania, 2000.
19. T. H. Shih, W. W. Liou, A. Shabbir, Z. Yang, and J. Zhu, A New $k - \epsilon$ Eddy Viscosity Model for High Reynolds Number Turbulent Flows, *Computer & Fluids*, vol. 24(3), pp. 227–238, 1995.
20. N. Peters, Laminar Diffusion Flamelet Models in Non-Premixed Turbulent Combustion, *Progress in Energy and Combustion Science*, vol. 10(3), pp. 319–339, 1984.
21. G. P. Smith, D. M. Golden, M. Frenklach, N. W. Moriarty, B. Eiteneer, M. Goldenberg, C. T. Bowman, R. K. Hanson, S. Song, W. C. Gardiner, and V. V. Z. Lissianski, Gri-Mech 3.0, Gas Research Institute, 1999.
22. E. M. Orbegoso, L. F. Figueira da Silva, and A. R. Novgorodcev Jr., On The Predictability of Chemical Kinetics for the Description of the Combustion of Simple Fuels, *Journal of the Brazilian Society of Mechanical Sciences & Engineering*, vol. 33(4), pp. 492-505, 2011.
23. L. Wang, N. E. Endrud, S. R. Turns, M. D. D'agostini, and A. G. Slavejkov, A Study of the Influence of Oxygen Index on Soot, Radiation, and Emission Characteristics of Turbulent Jet Flames, *Combustion Science and Technology*, vol. 174(8), pp. 45–72, 2002.
24. L. Wang, Detailed Chemistry, Soot, and Radiation Calculations in Turbulent Reacting Flows, PhD Thesis, The Pennsylvania State University, Pennsylvania, Pennsylvania, 2004.

25. L. Wang, D. C: Harworth, S. R. Turns, and M. F. Modest, Interactions among Soot, Thermal Radiation, and NO_x Emissions in Oxygen-Enriched Turbulent Non-Premixed Flames: A Computational Fluids Dynamics Modeling Study, *Combustion and Flame*, vol. 141(1-2), pp- 170–179, 2005.

List of Tables.

Table 1. Boundary conditions used for the simulation of Endrud [18] burner.

Table 2. Global properties obtained by the WSGGM(Smith)&Sazhin, WSGGM(Smith)&Rayleigh and NBM(Radcal) models. Sensible and radiative heat transfer rate at the longitudinal wall and Favre mean temperature at the exit of the computational domain.

Table 1. Boundary conditions used for the simulation of Endrud [18] burner.

BOUNDARY	PARAMETERS
Fuel Inlet	Fuel: Propane (C ₃ H ₈) $U_{z,0} = 21.8 \text{ m/s}^2$, (Re = 15 000), $I_t = \sqrt{u'^2}/\bar{U} = 3\%$, $l_t = 2 \text{ mm}$. $T_0 = 300 \text{ K}$, $X_{C_3H_8} = 1$, $\tilde{Z} = 1$, $\tilde{Z}''^2 = 0$. $\varepsilon_p = 0$ (Internal emissivity).
Oxidizer Inlet	Oxidizer: 40% of Oxygen (O ₂) and 60% of Nitrogen (H ₂) $U_{z,0} = 0.6 \text{ m/s}^2$, $I_t = \sqrt{u'^2}/\bar{U} = 3\%$, $l_t = 2 \text{ mm}$. $T_0 = 300 \text{ K}$, $X_{C_3H_8} = 1$, $\tilde{Z} = 0$, $\tilde{Z}''^2 = 0$. $\varepsilon_p = 0$ (Internal emissivity).
Walls	Type: Nonslip surface $T_0 = 300 \text{ K}$. $\varepsilon_p = 1$ (Internal emissivity).
Exit	$p_{exit} = 1 \text{ atm}$ $\varepsilon_p = 0$ (Internal emissivity).

Table 2. Global properties obtained by the WSGGM(Smith)&Sazhin, WSGGM(Smith)&Rayleigh and NBM(Radcal) models. Sensible and radiative heat transfer rate at the longitudinal wall and Favre mean temperature at the exit of the computational domain.

Property	WSGGM&Sazhin	WSGGM&Rayleigh	NBM(Radcal)	Experiment[21]
$\dot{Q}_{T,P}$ (W)	-95.3	-101.1	-96.0	-
$\dot{Q}_{r,P}$ (W)	-88.1	-94.8	-88.6	-72.36
\bar{T}_{exit} (K)	717	708	718	-

List of Figures.

Figure 1. Computational domain of the Endrud [18] burner composed by 92 540 hexaedrical control volumes.

Figure 2. Divergent of radiant heat flux obtained by the (a) WSGGM(Smith), WSGGM(Mossi) and NBM(Radcal) models and (b) the WSGGM(Smith)&Sazhin, WSGGM(Smith)&Rayleigh and NBM(Radcal) models. The results of (a) are compared with those obtained by Mossi [7] through LBL-HITEMP.

Figure 3. Divergent of radiant heat flux obtained at 1.5 and 1.8L using the (a) Narrow Band Model(Radcal) and, (b) Weigth Sum of Gray Gases. Both results are compared with those obtained by Mossi [7] through LBL-HITEMP approach.

Figure 4. Incident Radiation,G, obtained at 1.5 and 1.8L using the (a) Narrow Band Model(Radcal) and, (b) Weigth Sum of Gray Gases. Both results are compared with those obtained by Mossi [7] through LBL-HITEMP approach.

Figure 5. Mean absorption coefficient, a , obtained at 1.5 and 1.8L using the (a) Narrow Band Model(Radcal) and, (b) Weigth Sum of Gray Gases. Both results are compared with those obtained by Mossi [7] through LBL-HITEMP approach.

Figure 6. Comparisons of WSGGM(Smith) and WSGGM(Smith)&Sazhin models against the P1-FSK and P1-FSK&MM models and experimental data from Wang *et al.* [24, 25]. (a) Radiant heat flux and, (b) Equivalent soot volume fraction.

Figure 7. Comparisons of WSGGM(Smith)&Sazhin, WSGGM(Smith)&Rayleigh and NBM(Radcal) models against numerical and experimental data from Wang *et al.* [24, 25]. (a) Radiant heat flux and, (b) Equivalent soot volume fraction.

Figure 8. Contours of (a) soot volume fraction, (b) C₂H₂ and OH molar fraction, (c) soot surface growth rate, (d) soot oxidation rate and (e) overall formation rate, obtained with the WSGGM(Smith)&Sazhin model.

Figure 9. Influence of the oxidation scaling parameter, C_{oxid} , in the Moss-Brookes [15] model against the (a) Radiant heat flux and, (b) Equivalent soot volume fraction.

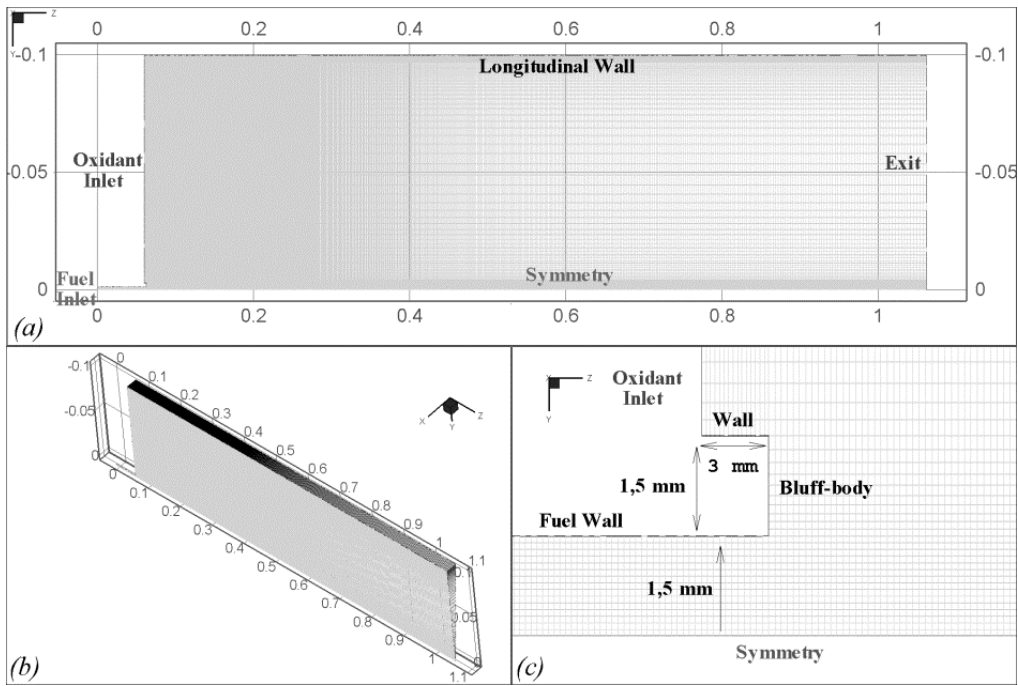


Figure 1. Computational domain of the Endrud [18] burner composed by 92 540 hexaedrical control volumes.

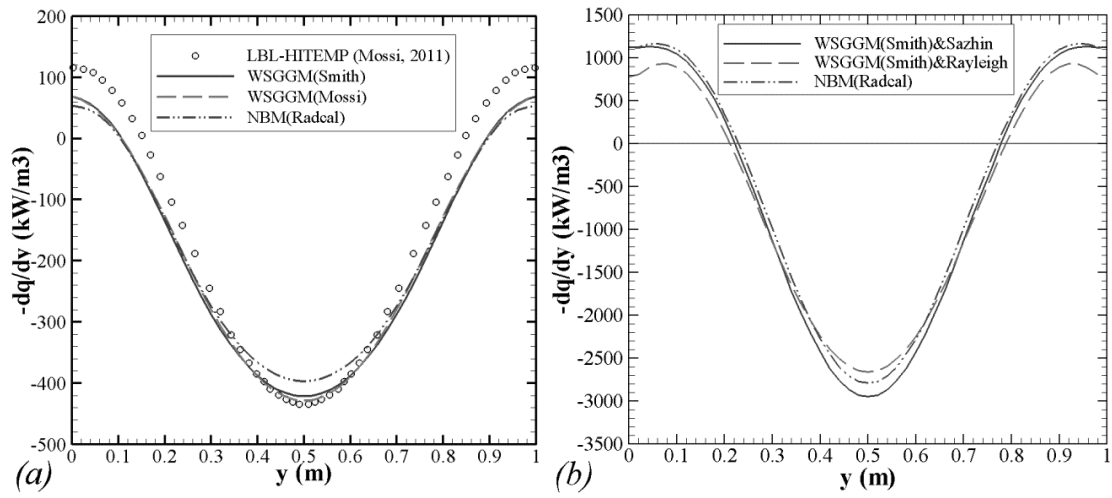


Figure 2. Divergent of radiant heat flux obtained by the (a) WSGGM(Smith), WSGGM(Mossi) and NBM(Radcal) models and (b) the WSGGM(Smith)&Sazhin, WSGGM(Smith)&Rayleigh and NBM(Radcal) models. The results of (a) are compared with those obtained by Mossi [7] through LBL-HITEMP.

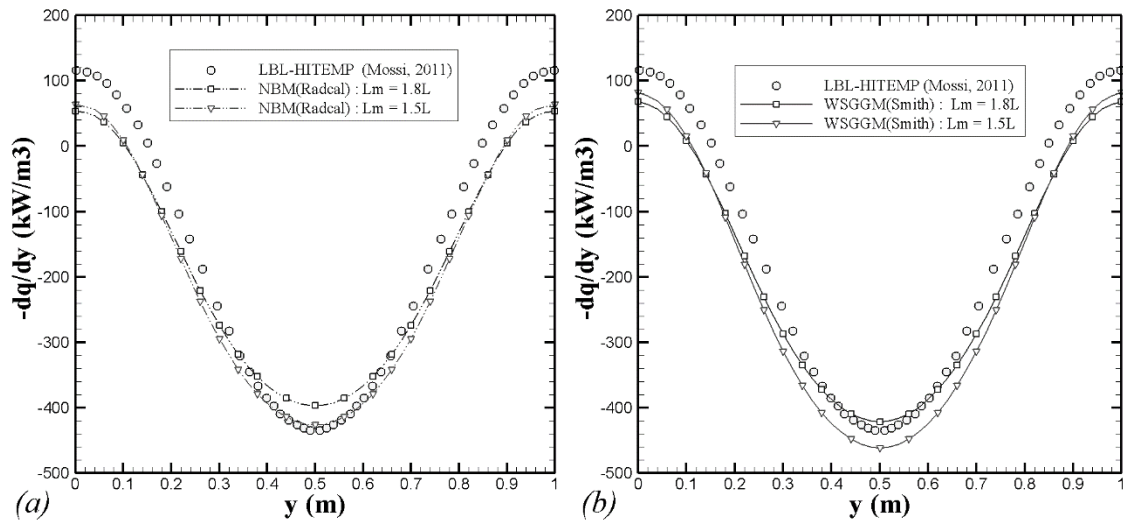


Figure 3. Divergent of radiant heat flux obtained at 1.5 and 1.8L using the (a) Narrow Band Model(Radcal) and, (b) Weigth Sum of Gray Gases. Both results are compared with those obtained by Mossi [7] through LBL-HITEMP approach.

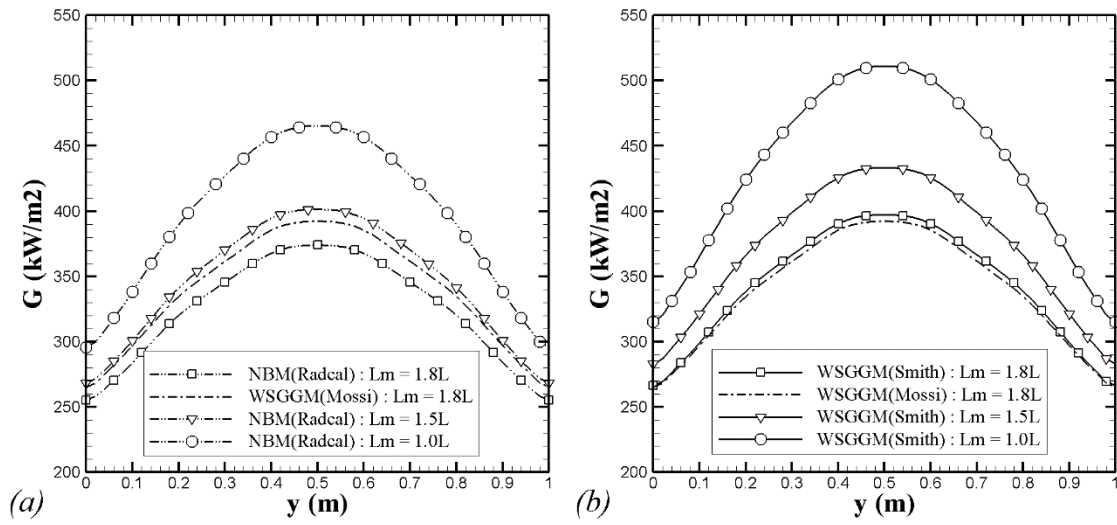


Figure 4. Incident Radiation, G , obtained at 1.5 and 1.8L using the (a) Narrow Band Model(Radcal) and, (b) Weight Sum of Gray Gases. Both results are compared with those obtained by Mossi [7] through LBL-HITEMP approach.

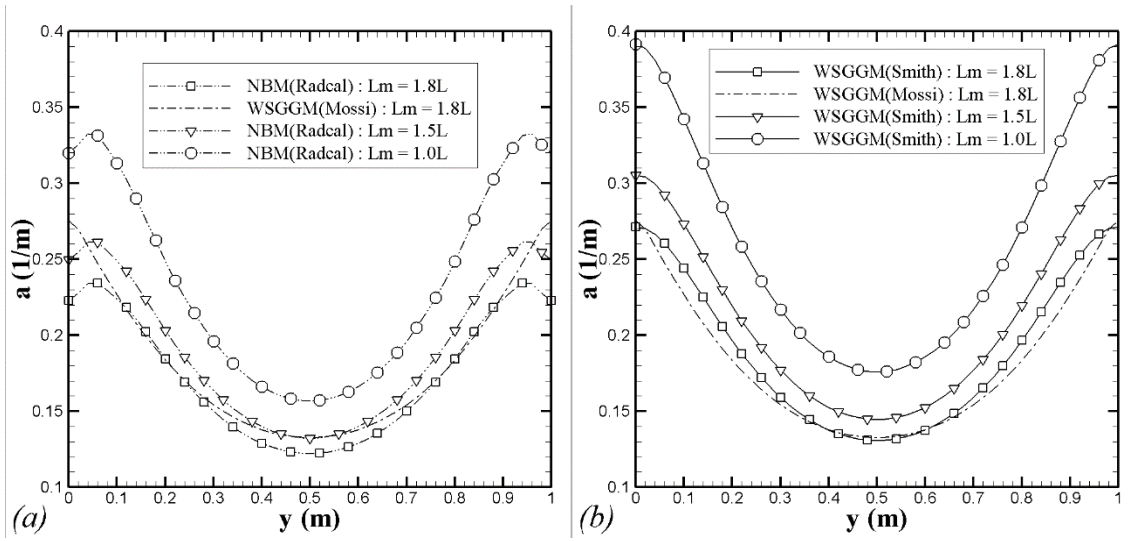


Figure 5. Mean absorption coefficient, a , obtained at 1.5 and 1.8L using the (a) Narrow Band Model(Radcal) and, (b) Weigh Sum of Gray Gases. Both results are compared with those obtained by Mossi [7] through LBL-HITEMP approach.

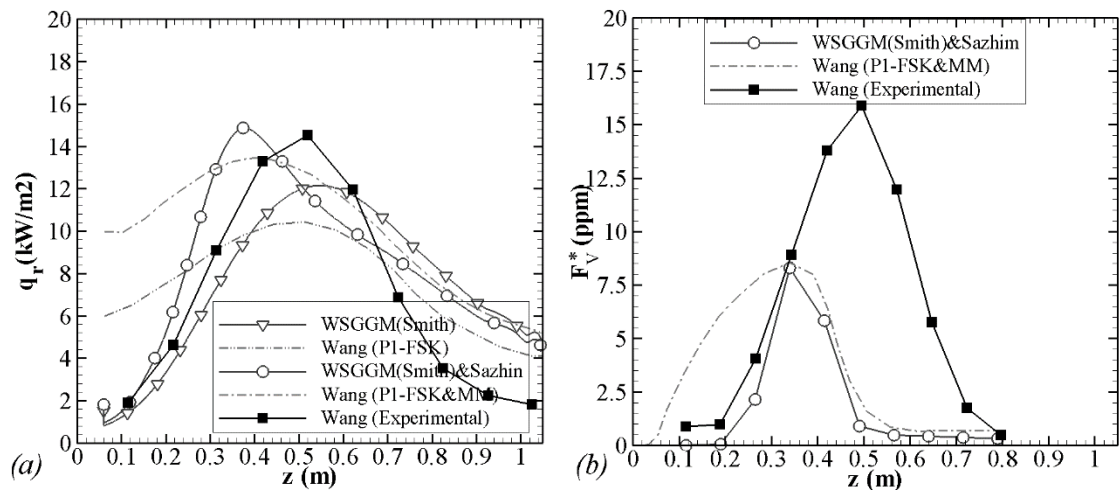


Figure 6. Comparisons of WSGGM(Smith) and WSGGM(Smith)&Sazhin models against the P1-FSK and P1-FSK&MM models and experimental data from Wang *et al.* [24, 25]. (a) Radiant heat flux and, (b) Equivalent soot volume fraction.

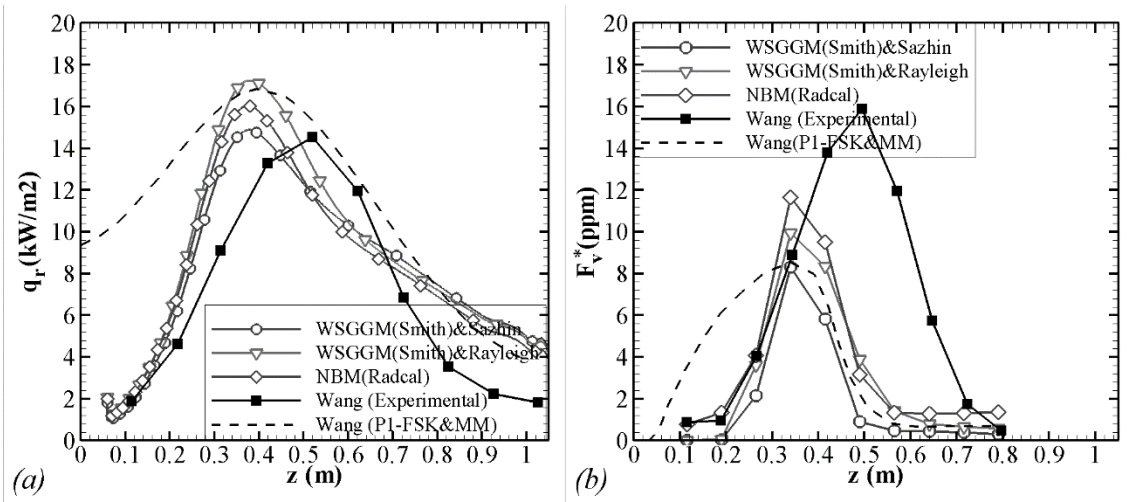


Figure 7. Comparisons of WSGGM(Smith)&Sazhin, WSGGM(Smith)&Rayleigh and NBM(Radcal) models against numerical and experimental data from Wang *et al.* [24, 25]. (a) Radiant heat flux and, (b) Equivalent soot volume fraction.

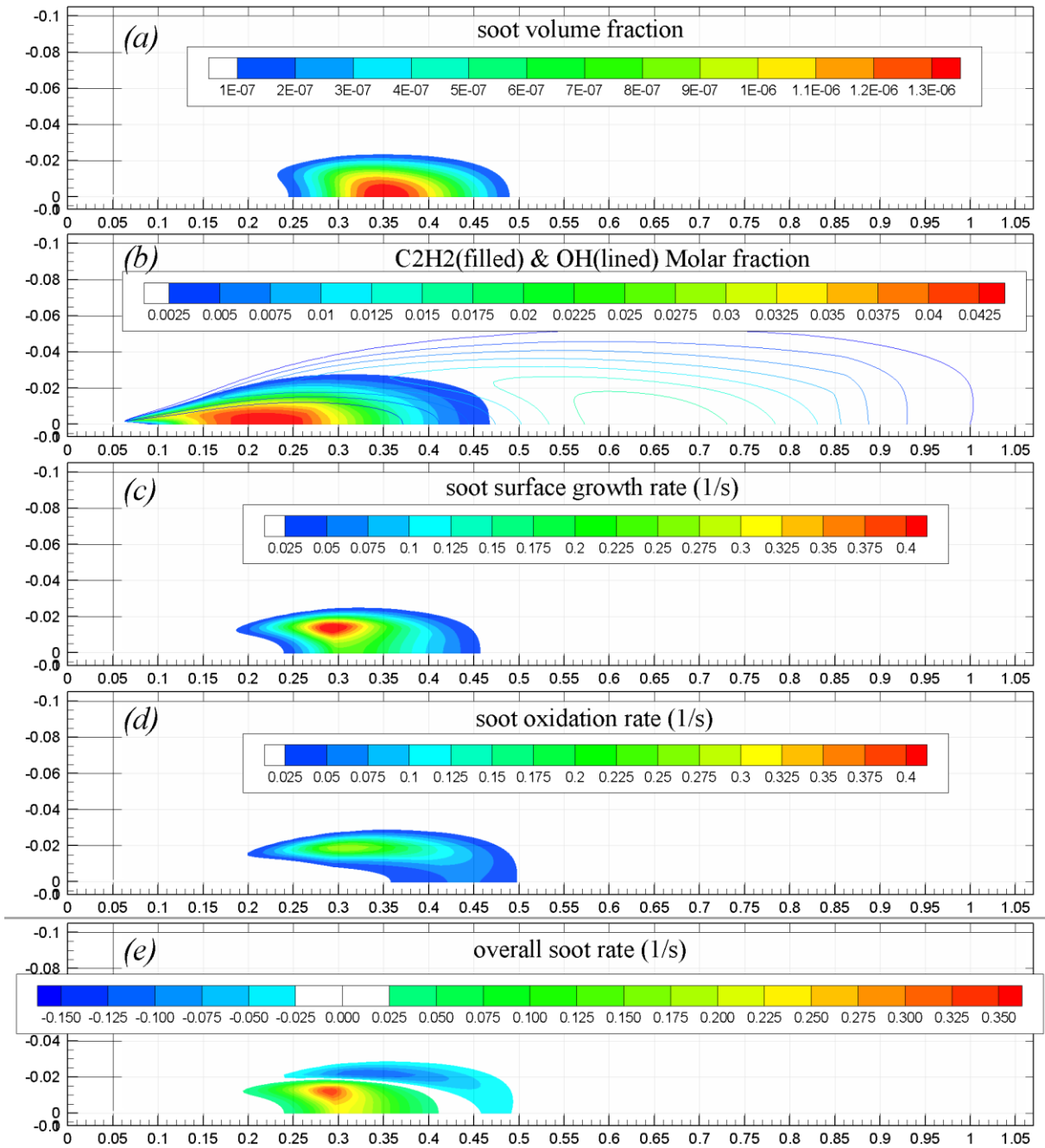


Figure 8. Contours of (a) soot volume fraction, (b) C2H2 and OH molar fraction, (c) soot surface growth rate, (d) soot oxidation rate and (e) overall formation rate, obtained with the WSGGM(Smith)&Sazhin model.

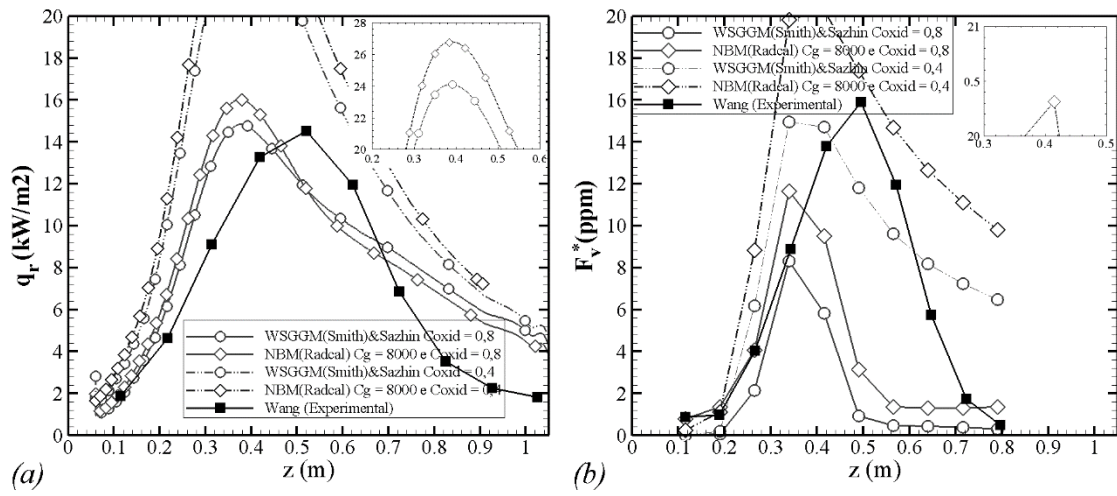


Figure 9. Influence of the oxidation scaling parameter, C_{oxid} , in the Moss-Brookes [15] model against the (a) Radiant heat flux and, (b) Equivalent soot volume fraction.